

Inclusion of Instantaneous Influences in the Spectral Decomposition of Causality: Application to the Control Mechanisms of Heart Rate Variability

Davide Nuzzi*, Luca Faes†, Michal Javorka‡, Daniele Marinazzo§ and Sebastiano Stramaglia*

* Dipartimento Interateneo di Fisica, Università degli Studi Aldo Moro di Bari
INFN, sezione di Bari, 70126, Bari, Italy

Email: davide.nuzzi@uniba.it, sebastiano.stramaglia@uniba.it

† Dipartimento di Ingegneria, Università di Palermo, 90128, Palermo
Email: luca.faes@unipa.it

‡ Department of Physiology, Cornelius University in Bratislava, 0361 Martin, Slovakia
Email: mjavorka@jfmed.uniba.sk

§ Department of Data Analysis, Ghent University, 9000 Ghent, Belgium
Email: daniele.marinazzo@gmail.com

Abstract—Heart rate variability is the result of several physiological regulation mechanisms, including cardiovascular and cardiorespiratory interactions. Since instantaneous influences occurring within the same cardiac beat are commonplace in this regulation, their inclusion is mandatory to get a realistic model of physiological causal interactions. Here we exploit a recently proposed framework for the spectral decomposition of causal influences between autoregressive processes [2] and generalize it by introducing instantaneous couplings in the vector autoregressive model (VAR). We show the effectiveness of the proposed approach on a toy model, and on real data consisting of heart period (RR), systolic pressure (SAP) and respiration (RESP) variability series measured in healthy subjects in baseline and head up tilt conditions. In particular, we show that our framework allows one to highlight patterns of frequency domain causality that are consistent with well-interpretable physiological interaction mechanisms like the weakening of respiratory sinus arrhythmia at high frequencies and the activation of the baroreflex control at lower frequencies, in response to postural stress.

Index Terms—Network physiology, Regression analysis, Spectral analysis, Stochastic processes.

I. INTRODUCTION

Vector autoregressive (VAR) models are ubiquitously used to quantify the concept of Granger causality (GC) between coupled processes in the time and frequency domains [1]. While causality is defined with regard to time-lagged effects between coupled processes, the existence of instantaneous (zero-lag) influences is typical in the analysis of real world time series, and its neglect has an impact on the proper assessment of GC measures [5]. Here, we consider a recently proposed framework for the spectral decomposition of causal influences between VAR processes [2] and generalize it by introducing instantaneous couplings in the associated VAR model. This allows us (i) to handle applications where instantaneous influences are expected, like in the cardiovascular and cardiorespiratory regulation system, and (ii) to derive the connectivity matrices of the full and disconnected models

to be defined for GC computation by solving Yule-Walker like equations, whose only inputs are the correlation matrices of the original data. According to the frame introduced in [2], the causal influences evaluated by our approach can be expressed in the time domain or in the frequency domain. Instantaneous causality may describe either fast (within-sample) physiological interactions or other effects due to unobserved confounders. We argue that our framework, including instantaneous effects both in the time and the frequency domain, may help reveal physiologically relevant mechanisms and to ascribe them to the correct frequency band.

The paper is organized as follows. In the next Section we describe the formalism and motivate our approach. In Section III we show the application of the proposed methodology on a simulated toy model mimicking the human cardiovascular and respiratory dynamics. In Section IV we analyze real data consisting of heart period (RR interval of the ECG), systolic arterial pressure (SAP) and respiration (RESP) variability time series measured from healthy subjects monitored in the supine rest and head-up tilt conditions. Some conclusions are drawn in Section V.

II. TIME AND FREQUENCY DOMAIN MEASURES OF INFORMATION TRANSFER FOR VECTOR AUTOREGRESSIVE PROCESSES WITH INSTANTANEOUS EFFECTS

In order to quantify the information transfer from RESP and SAP processes (sources) to the RR process (target) we exploit the framework of information dynamics, where the directed transfer of information between interacting processes is quantified by the transfer entropy (TE). The information that each source transfers individually to the target, here denoted as pairwise TE, is defined as

$$\mathcal{T}_{\text{RESP} \rightarrow \text{RR}} = I(\text{RR}_t; \text{RESP}_t^- | \text{RR}_t^-), \quad (1)$$

$$\mathcal{T}_{\text{SAP} \rightarrow \text{RR}} = I(\text{RR}_t; \text{SAP}_t^- | \text{RR}_t^-), \quad (2)$$

where $I(\cdot; \cdot | \cdot)$ denotes the conditional mutual information, RR_t is the state of process RR at time t and $\text{RESP}_t^-, \text{SAP}_t^-, \text{RR}_t^-$ are the past states of RESP, SAP and RR respectively. Since the pairwise TE from one source to the target may include information that is mediated by the other source, to quantify the transfer of information with focus on one specific source we introduce the conditional TE defined as

$$\mathcal{T}_{\text{RESP} \rightarrow \text{RR} | \text{SAP}} = I(\text{RR}_t; \text{RESP}_t^- | \text{RR}_t^-, \text{SAP}_t^-), \quad (3)$$

$$\mathcal{T}_{\text{SAP} \rightarrow \text{RR} | \text{RESP}} = I(\text{RR}_t; \text{SAP}_t^- | \text{RR}_t^-, \text{RESP}_t^-). \quad (4)$$

These TE definitions only account for lagged interactions, but for the processes in question it is useful to introduce also instantaneous interactions between the source processes and the target. This can be done including the present state of the source process inside the past vector, i.e. considering $\text{RESP}_{t+1}^- = (\text{RESP}_t, \text{RESP}_{t-1}, \dots)$ and $\text{SAP}_{t+1}^- = (\text{SAP}_t, \text{SAP}_{t-1}, \dots)$ in the above equations.

The frequency domain representation of pairwise and conditional TE can be obtained describing the multivariate process as a vector autoregressive process (VAR) of order p that includes instantaneous interactions [5]

$$\mathbf{x}_t = \sum_{k=0}^p B_k \mathbf{x}_{t-k} + \boldsymbol{\eta}_t, \quad (5)$$

where the state of the system at time t is described by the vector $\mathbf{x}_t = (\text{RESP}_t, \text{SAP}_t, \text{RR}_t)$, the matrices $B_{k>0}$ are called *connectivity matrices* and contain the coupling coefficients between each process at time t and every other process k steps in the past. The matrix B_0 contains the instantaneous couplings and must be a lower (or upper) triangular matrix in order to induce an acyclic instantaneous interaction graph. The vector $\boldsymbol{\eta}_t$ represents normally distributed residuals that are uncorrelated over time, whose covariance matrix is denoted as $\Sigma = \mathbb{E}[\boldsymbol{\eta}_t \boldsymbol{\eta}_t^T]$. The choice to include instantaneous interactions in B_0 guarantees that Σ will be a diagonal matrix.

We can evaluate Σ using (5) and we get

$$\Sigma = \Gamma_0 - \sum_{l=0}^p \Gamma_l B_l^T - \sum_{l=0}^p B_l \Gamma_l^T + \sum_{l=0}^p \sum_{k=0}^p B_l \Gamma_{k-l} B_k^T, \quad (6)$$

where the $\Gamma_k = \mathbb{E}[\mathbf{x}_t \mathbf{x}_{t-k}^T]$ are the correlations matrices of the process. The accuracy of predicting the present state \mathbf{x}_t given all the past states \mathbf{x}_{t-k} can be quantified by the determinant $|\Sigma|$, which is called the *generalized variance*. The connectivity matrices B_k that minimize the generalized variance are obtained differentiating $|\Sigma|$ with respect to all the components of each connectivity matrix $(B_k)_{ij}$, leading to the equation

$$\frac{d|\Sigma|}{d(B_k)_{ij}} = 2|\Sigma| \left[\Sigma^{-1} \left(\sum_{l=0}^p B_l \Gamma_{k-l} - \Gamma_k \right) \right]_{ij} = 0, \quad (7)$$

for each $k = 0, 1, \dots, p$. This equation should be solved for the coefficients $(B_k)_{ij}$; note that since some coefficients of

B_0 are fixed and vanishing, optimization would require the use of numerical methods (like the gradient descent).

If we didn't choose to include the instantaneous connectivity matrix B_0 into the model we could solve for each $i, j = 1 \dots N$, where N is the number of processes under consideration, and (7) would simplify to

$$\sum_{l=1}^p B_l \Gamma_{k-l} - \Gamma_k = 0, \quad (8)$$

that are the well-known Yule-Walker equations.

On the other hand, our choice to include instantaneous couplings renders Σ diagonal, thus allowing us to simplify (7) to

$$\left(\sum_{l=0}^p B_l \Gamma_{k-l} - \Gamma_k \right)_{ij} = 0. \quad (9)$$

We stress that these equations resemble the classical Yule Walker, and can be rewritten as a matrix inversion problem; details will be given elsewhere.

As in [2] we introduce now a new model, the *disconnected model*, where some of the interactions are *cut*, i.e. where the couplings from a source j to a target i are forced to zero in all the connectivity matrices, including instantaneous couplings. The new connectivity matrices and the residuals covariance matrix will be denoted as B'_k and Σ' respectively. The minimization of the generalized variance $|\Sigma'|$ with respect to $(B'_k)_{ij}$ leads to (7), for the new variables. Then, since for the disconnected model Σ' may not be a diagonal matrix, following [2] we choose to solve (9) for the $(B'_k)_{ij}$ coefficients as if Σ' were diagonal, and then evaluate it using (6), keeping only the diagonal terms and forcing the off-diagonal terms to zero.

The information transfer from process j to process i can now be quantified as

$$\mathcal{T}_{j \rightarrow i} = \frac{1}{2} \log \left(\frac{|\Sigma'|}{|\Sigma|} \right). \quad (10)$$

This measure is called Granger Causality (GC) [3] and it has been shown in [4] that it is equivalent to TE for multivariate gaussian processes. The choice to neglect the off-diagonal terms of Σ' can be interpreted as a way of quantifying the contribution of instantaneous information transfer from j to i that could not be described just by forcing the value of $(B_0)_{ij}$ to zero. Moving to the frequency domain, we derive the spectral decomposition for each TE as

$$\tilde{\mathcal{T}}_{j \rightarrow i}(\omega) = \frac{1}{2} \log \left(\frac{|S'(\omega)|}{|S(\omega)|} \right), \quad (11)$$

where $S(\omega)$ and $S'(\omega)$ are the spectral density matrices of the full and disconnected model respectively. For VAR processes, the spectral density matrix can be evaluated as $S(\omega) = H(\omega) \Sigma H(\omega)^\dagger$, where $H(\omega)$ is the transfer matrix defined as $H(\omega) = (\mathbb{I} - \sum_{k=0}^p B_k e^{-i\omega k})^{-1}$; $S'(\omega)$ can be evaluated using the covariance matrix Σ' and the connectivity matrices B'_k leading to the transfer matrix $H'(\omega)$. For stable

VAR models [7] the time-domain TE can be recovered through integration

$$\mathcal{T}_{j \rightarrow i} = \frac{1}{2\pi} \int_{-\pi}^{\pi} \tilde{\mathcal{T}}_{j \rightarrow i}(\omega). \quad (12)$$

Our approach can be used to evaluate both the pairwise and conditional TE, with and without instantaneous information transfer, in a fast and efficient way. The workflow can be summarized as follows:

- The optimal model order p is evaluated for the full multivariate model using the AIC or BIC criterion [6].
- Ordinary least squares (OLS) is used, in conjunction with the Yule-Walker equations, in order to obtain the correlation matrices Γ_k for $k = 0 \dots q$, with $q > p$.
- The full model coefficients B_k are evaluated using (9) and the corresponding covariance matrix Σ using (6), preserving only the diagonal elements.
- The disconnected model coefficients B'_k are calculated using (9), forcing the desired causal influences to zero. The corresponding covariance matrix Σ' is obtained like in the previous step.
- The time-domain TE is evaluated using (10).
- The spectral density matrices $S(\omega)$ and $S'(\omega)$ are evaluated for the full and disconnected models, from which the frequency-domain TE can be evaluated using (11).

In order to evaluate the pairwise TE from a single source j to a target i , all the couplings from the other sources must be cut in both the full and disconnected model.

III. VALIDATION ON SIMULATED TIME SERIES

We test our framework on simulated RESP, SAP and RR time series obtained using a VAR(2) model. The lagged connectivity matrices are

$$B_1 = \begin{pmatrix} 2r_1 \cos \theta_1 & 0 & 0 \\ b_{21}^1 & 2r_2 \cos \theta_2 & 0 \\ b_{31}^1 & b_{32}^1 & 2r_3 \cos \theta_3 \end{pmatrix}, \quad (13)$$

$$B_2 = \begin{pmatrix} -r_1^2 & 0 & 0 \\ b_{21}^2 & -r_2^2 & 0 \\ b_{31}^2 & b_{32}^2 & -r_3^2 \end{pmatrix}, \quad (14)$$

where $r_1 = 0.9, r_2 = 0.8, r_3 = 0.55$ and $\theta_i = 2\pi f_i$ (assuming a sampling frequency of 1 Hz). The oscillatory frequencies are chosen as $f_1 = 0.3$ Hz for the RESP process, $f_2 = 0.1$ Hz for the SAP process and $f_3 = 0.02$ Hz for the RR process, in order to replicate the HF, LF and VLF oscillations found in real RR spectra [8]. The coupling coefficients at lag 1 are chosen as $b_{21}^1 = 0.3, b_{31}^1 = 0.2$ and $b_{32}^1 = 0.25$, while the coefficients at lag 2 are chosen as $b_{ij}^2 = -2b_{ij}^1$. The residuals covariance matrix is chosen as the unit matrix.

In the first simulation we neglect instantaneous effects by setting $B_0 = 0$ and generate 20 realizations of the multivariate stochastic process with length $T = 300$ samples. Figure (1) shows an example of the resulting time series for RESP, SAP and RR and their power spectra. We then evaluate the pairwise and conditional TEs in the frequency domain, taking RESP and SAP as sources and RR as target, with and without

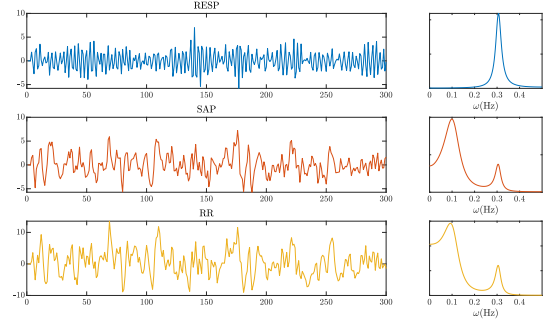


Fig. 1. Left: RESP, SAP and RR time series simulated using the VAR(2) model with coefficients in (13,14). Right: The corresponding power spectra.

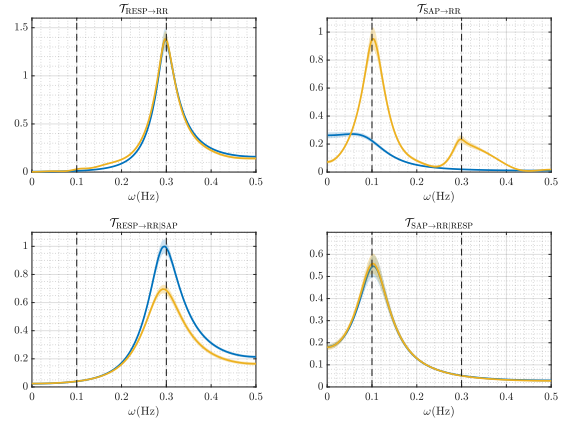


Fig. 2. Pairwise and conditional TEs in the frequency domain for the time series simulated without instantaneous interactions. The blue curves (—) represent only the lagged contributions to information transfer, while the yellow curves (—) include instantaneous contributions. The dashed lines indicate the oscillatory frequency for the RESP and SAP signals. $\tilde{\mathcal{T}}_{SAP \rightarrow RR}$ is different because the delayed interactions $RESP \rightarrow RR$ and $RESP \rightarrow SAP$ in the multivariate model create a fictitious instantaneous interaction between SAP and RR. $\tilde{\mathcal{T}}_{RESP \rightarrow RR|SAP}$ is lower when considering instantaneous interactions because in the disconnected model some of the influence of RESP is mediated by instantaneous interactions between SAP and RR.

instantaneous information transfer. The model order is $p = 2$ and the correlation matrices Γ_k are evaluated up to $q = 50$. The full model connectivity matrices B_k are evaluated up to order 2 for the conditional TE and up to order 10 for the pairwise TE. The disconnected model connectivity matrices are all evaluated up to order 50.

The results, depicted in Figure (2), show that $\tilde{\mathcal{T}}_{RESP \rightarrow RR}$ peaks exactly at 0.3 Hz and there is no contribution from instantaneous information transfer. The same is true for $\tilde{\mathcal{T}}_{SAP \rightarrow RR|RESP}$, that peaks at the frequency of 0.1 Hz. The other two measures show a difference between the model with instantaneous interaction and the model without them: $\tilde{\mathcal{T}}_{RESP \rightarrow RR|SAP}$ is lower when considering instantaneous interactions because in the disconnected model some of the influence from RESP to RR is already accounted for in the instantaneous interactions between SAP and RR. The fact that RESP influences directly both SAP and RR gives rise to strong

instantaneous contributions from SAP to RR, that explain the difference between the two curves for $\tilde{\mathcal{T}}_{\text{SAP} \rightarrow \text{RR}}$ and the well defined peak at 0.3Hz.

In the second simulation we introduce instantaneous couplings in the simulated data using the connectivity matrix

$$B_0 = \begin{pmatrix} 0 & 0 & 0 \\ 1.5 & 0 & 0 \\ 0.5 & 0 & 0 \end{pmatrix}. \quad (15)$$

The pairwise and conditional spectral TE are shown in Figure (3); the model without instantaneous interactions fails to identify the peaks of information transfer except for the $\tilde{\mathcal{T}}_{\text{SAP} \rightarrow \text{RR}|\text{RESP}}$, where there are no instantaneous contributions from SAP to RR if the effects of RESP are taken into consideration. In $\tilde{\mathcal{T}}_{\text{SAP} \rightarrow \text{RR}}$ it can be seen that the peak at 0.3Hz is enhanced by the strong instantaneous couplings from RESP to SAP and RR.

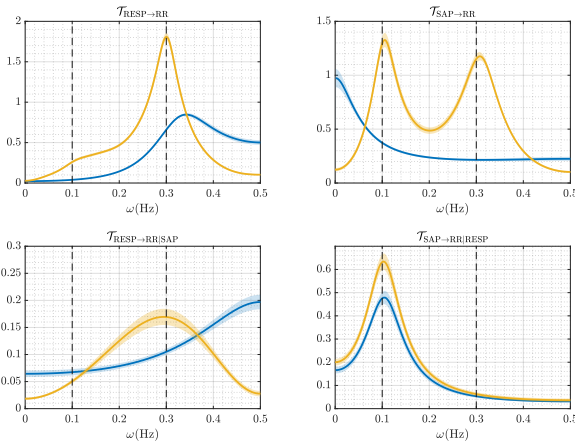


Fig. 3. Pairwise and conditional TEs in the frequency domain for the simulated time series that includes instantaneous interactions. The blue curves (—) represent only the lagged contributions to information transfer, while the yellow curves (—) include instantaneous contributions. The dashed lines indicate the oscillatory frequency for the RESP and SAP signals. The inclusion of instantaneous interactions allows to locate information transfer at the frequencies specific of the oscillatory content of the simulated process.

IV. APPLICATION TO CARDIOVASCULAR AND RESPIRATORY VARIABILITY SERIES

We analyze a dataset of cardiovascular and respiratory time series previously collected [8], where 61 young healthy subjects were monitored in the resting supine condition (REST) and in the upright position reached after passive head-up tilt (HUT). The recorded signals were the electrocardiogram (ECG, lead II), the finger arterial pressure signal (Finapres device) and the respiration signal acquired through inductive plethysmography. From these signals, the time series of RR, SAP and RESP were measured respectively taking the consecutive interbeat interval durations from the ECG, the local maxima of the arterial pressure inside each detected RR interval, and values of the respiration signal sampled at the onset of each detected RR interval. Synchronous time

series of 300 points, free of artifacts and satisfying stationarity criteria, were selected for the analysis in the two conditions. Note that the adopted measurement convention implicitly sets instantaneous (within-beat) interactions from RESP to SAP and RR, and from SAP to RR. All the TE are calculated using a model order of $p = 5$ and the correlation matrices Γ_k are evaluated up to $q = 50$ for all the subjects. The full model connectivity matrices B_k are evaluated up to order 5 for the conditional TE and up to order 10 for the pairwise TE. The disconnected model connectivity matrices are all evaluated up to order 50.

We also integrated each spectral TE in two frequency bands: the LF band ($[0.04, 0.15]$ Hz) and the HF band ($[0.15, 0.4]$ Hz) [9]. Figure (4) depicts the distribution across subjects of each information measure, computed with and without considering the instantaneous information transfer and assessed separately for the two frequency bands in both the REST and HUT conditions. Statistically significant differences between the two phases or between the two approaches used to calculate the TE are shown as lines connecting the relevant pairs of distributions. Each statistical comparison is carried out using the Wilcoxon signed-rank test and the corresponding effect size is expressed as Kendall's W, choosing a significance level $\alpha = 0.05$. The results of the comparison between the two phases are shown in Table (I), while the comparison between the two methods is shown in Table (II); the p -values in bold denote a significant difference.

In the LF band the $\mathcal{T}_{\text{RESP} \rightarrow \text{RR}}$, $\mathcal{T}_{\text{SAP} \rightarrow \text{RR}}$ and $\mathcal{T}_{\text{SAP} \rightarrow \text{RR}|\text{RESP}}$ are significantly higher in the HUT phase than in the rest phase, for both methods. The increased information transfer from SAP to RR during HUT is expected as it reflects the well-known activation of the baroreflex mechanism whereby LF pressure oscillations are transmitted to the heart rate as a response to the postural stress [10]. In general, we find that including instantaneous effects increases the LF values of the information transfer from SAP to RR, and decreases the LF values of the information transfer from RESP to RR. These results document the importance and appropriateness of considering instantaneous effects in the analysis of cardiovascular interactions, where zero-lag effects are expected to contribute significantly to the baroreflex mechanism [5], and of cardiorespiratory interactions, where negligible information transfer is expected to occur from RESP to RR in the LF band [11].

In the HF band there is a significant increase in $\mathcal{T}_{\text{SAP} \rightarrow \text{RR}}$ and $\mathcal{T}_{\text{SAP} \rightarrow \text{RR}|\text{RESP}}$ between the supine rest phase and the HUT phase, but only if we neglect instantaneous effects; this suggests that baroreflex activation resulting in a stronger transfer of information from SAP to RR is actually active only in the LF band [5], [10], while finding it in the HF band is indicative of inappropriate modelling of the instantaneous effects. On the other hand $\mathcal{T}_{\text{RESP} \rightarrow \text{RR}|\text{SAP}}$ decreases significantly from rest to tilt when zero-lag effects are modeled. This decrease, which has been previously documented and reflects a weakening of the respiratory sinus arrhythmia during tilt [11], can be documented only when we account for the instantaneous

TABLE I
SUPINE REST VS. HUT

| No instant | LF | | HF | |
|--|------------------|-------------|------------------|-------------|
| | p Value | Kendall W | p Value | Kendall W |
| $\mathcal{T}_{\text{RESP} \rightarrow \text{RR}}$ | 0.03 | 0.078 | 0.899 | 0 |
| $\mathcal{T}_{\text{SAP} \rightarrow \text{RR}}$ | <0.001 | 0.226 | 0.003 | 0.142 |
| $\mathcal{T}_{\text{RESP} \rightarrow \text{RR} \text{SAP}}$ | 0.030 | 0.078 | 0.055 | 0.061 |
| $\mathcal{T}_{\text{SAP} \rightarrow \text{RR} \text{RESP}}$ | <0.001 | 0.368 | <0.001 | 0.226 |
| With instant | LF | | HF | |
| | p Value | Kendall W | p Value | Kendall W |
| $\mathcal{T}_{\text{RESP} \rightarrow \text{RR}}$ | 0.003 | 0.142 | 0.250 | 0.022 |
| $\mathcal{T}_{\text{SAP} \rightarrow \text{RR}}$ | <0.001 | 0.409 | 0.250 | 0.022 |
| $\mathcal{T}_{\text{RESP} \rightarrow \text{RR} \text{SAP}}$ | 0.522 | 0.007 | 0.015 | 0.097 |
| $\mathcal{T}_{\text{SAP} \rightarrow \text{RR} \text{RESP}}$ | <0.001 | 0.409 | 0.522 | 0.007 |

TABLE II
WITH VS. WITHOUT INSTANTANEOUS INTERACTIONS

| Supine rest | LF | | HF | |
|--|------------------|-------------|------------------|-------------|
| | p Value | Kendall W | p Value | Kendall W |
| $\mathcal{T}_{\text{RESP} \rightarrow \text{RR}}$ | <0.001 | 0.329 | <0.001 | 0.368 |
| $\mathcal{T}_{\text{SAP} \rightarrow \text{RR}}$ | <0.001 | 0.645 | <0.001 | 0.873 |
| $\mathcal{T}_{\text{RESP} \rightarrow \text{RR} \text{SAP}}$ | <0.001 | 0.409 | 0.923 | 0.007 |
| $\mathcal{T}_{\text{SAP} \rightarrow \text{RR} \text{RESP}}$ | <0.001 | 0.409 | <0.001 | 0.329 |
| HUT | LF | | HF | |
| | p Value | Kendall W | p Value | Kendall W |
| $\mathcal{T}_{\text{RESP} \rightarrow \text{RR}}$ | <0.001 | 0.645 | <0.001 | 0.293 |
| $\mathcal{T}_{\text{SAP} \rightarrow \text{RR}}$ | <0.001 | 0.873 | <0.001 | 0.258 |
| $\mathcal{T}_{\text{RESP} \rightarrow \text{RR} \text{SAP}}$ | 0.118 | 0.002 | 0.991 | 0.007 |
| $\mathcal{T}_{\text{SAP} \rightarrow \text{RR} \text{RESP}}$ | <0.001 | 0.645 | 0.243 | 0.013 |

V. CONCLUSIONS

We have proposed the inclusion of instantaneous effects in the framework for the spectral decomposition of causal influences between autoregressive processes described in [2]. Our treatment shows how causality can be analytically obtained from a single-fit of the full model and the subsequent derivation of the disconnected models needed for the evaluation of frequency domain GC. The application to an analysis domain where instantaneous influences between time series are physiologically relevant has shown the appropriateness of the extended framework to describe expected regulatory mechanisms which operate in specific and distinct frequency bands; these include the weakening of respiratory sinus arrhythmia at the respiratory frequencies, and the activation of the baroreflex control of the heart rate at lower frequencies, in response to postural stress. Our new approach may be useful in the construction of indexes that may act as warning signs of worsening heart failure.

REFERENCES

[1] Barnett, Lionel, and Anil K. Seth. "The MVGC multivariate Granger causality toolbox: a new approach to Granger-causal inference." *Journal of neuroscience methods* 223 (2014): 50-68.

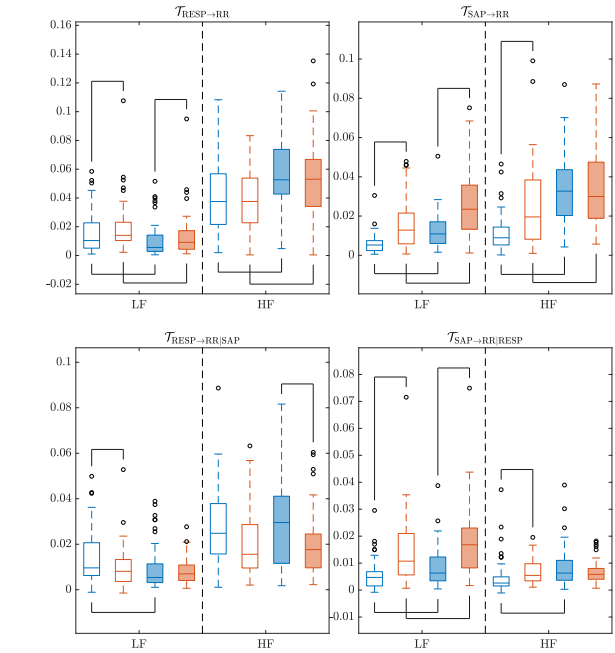


Fig. 4. Spectral pairwise and conditional TEs integrated over the low frequency (LF) range [0.04, 0.15]Hz and over the high frequency (HF) range [0.15, 0.4]Hz. Blue (\square) and orange (\square) boxes correspond to REST and HUT phases respectively. Empty boxes correspond to the model without instantaneous information transfer, while filled boxes correspond to the model that considers both instantaneous and lagged information transfer. Boxes are connected if there is a statistically significant difference between the respective measures.

[2] Cohen, D., Sasai, S., Tsuchiya, N., and Oizumi, M. (2020). A general spectral decomposition of causal influences applied to integrated information. *Journal of neuroscience methods*, 330, 108443.

[3] Barnett, Adam B., Lionel Barnett, and Anil K. Seth. "Multivariate Granger causality and generalized variance." *Physical Review E* 81.4 (2010): 041907.

[4] Barnett, Lionel, Adam B. Barnett, and Anil K. Seth. "Granger causality and transfer entropy are equivalent for Gaussian variables." *Physical review letters* 103.23 (2009): 238701.

[5] Faes, Luca, et al. "A framework for assessing frequency domain causality in physiological time series with instantaneous effects." *Philosophical Transactions of the Royal Society A: Mathematical, Physical and Engineering Sciences* 371.1997 (2013): 20110618.

[6] McQuarrie, Allan DR, and Chih-Ling Tsai. *Regression and time series model selection*. World Scientific, 1998.

[7] Geweke, John. "Measurement of linear dependence and feedback between multiple time series." *Journal of the American statistical association* 77.378 (1982): 304-313.

[8] Krohova, Jana, et al. "Multiscale information decomposition dissects control mechanisms of heart rate variability at rest and during physiological stress." *Entropy* 21.5 (2019): 526.

[9] Berntson, Gary G., et al. "Heart rate variability: origins, methods, and interpretive caveats." *Psychophysiology* 34.6 (1997): 623-648.

[10] Faes, Luca, Giandomenico Nollo, and Alberto Porta. "Mechanisms of causal interaction between short-term RR interval and systolic arterial pressure oscillations during orthostatic challenge." *Journal of Applied Physiology* 114.12 (2013): 1657-1667.

[11] Faes, Luca, Giandomenico Nollo, and Alberto Porta. "Non-uniform multivariate embedding to assess the information transfer in cardiovascular and cardiorespiratory variability series." *Computers in biology and medicine* 42.3 (2012): 290-297.